arXiv:2002.08053v3 [cs.LG] 5 Sep 2020

Progressive Identification of True Labels for Partial-Label Learning

Jiaqi Lv [†1] **Miao Xu** [2 3] **Lei Feng** [4] **Gang Niu** [2] **Xin Geng** [1] **Masashi Sugiyama** [2 5]

Abstract

Partial-label learning (PLL) is a typical weakly supervised learning problem, where each training instance is equipped with a set of candidate labels among which only one is the true label. Most existing methods elaborately designed learning objectives as constrained optimizations that must be solved in specific manners, making their computational complexity a bottleneck for *scaling up to big data*. The goal of this paper is to propose a novel framework of PLL *with flexibility on the model and optimization algorithm*. More specifically, we propose a novel estimator of the classification risk, theoretically analyze the *classifier-consistency*, and establish an estimation error bound. Then we propose a *progressive identification* algorithm for approximately minimizing the proposed risk estimator, where the update of the model and identification of true labels are conducted in a seamless manner. The resulting algorithm is model-independent and loss-independent, and compatible with stochastic optimization. Thorough experiments demonstrate it sets the new state of the art.

1. Introduction

The increasing demand for massive data used in training modern machine learning models, such as deep neural networks (DNNs), makes it inevitable that not all examples are equipped with strong supervision information. Weak supervision may result in a detrimental effect on model training and has been widely studied (Zhou, 2017; Patrini et al., 2017; Kamnitsas et al., 2018; Lu et al., 2019; Gong et al., 2019). We focus on an important weakly supervised learning problem called *partial-label learning* (PLL) (Cour et al., 2011; Wang et al., 2019; Lyu et al., 2019), where each training instance is associated with *a set of candidate labels* among which *exactly one* is true, reducing the overhead of finding exact label from ambiguous candidates. This problem arises in many real-world tasks such as automatic image annotation (Chen et al., 2018), web mining (Luo & Orabona, 2010), etc.

Related research on PLL was pioneered by a *multiple-label learning* (MLL) method (Jin & Ghahramani, 2003). Despite the same form of supervision information, i.e., a set of candidate labels, that each training instance is assigned with, a vital difference between MLL and PLL is that the goal of PLL is identifying the *only one* true label among candidate labels whereas for MLL identifying an *arbitrary* label in the candidate label set is acceptable, i.e., treating all candidate labels equally. In practice, Jin & Ghahramani (2003) formulated an *unconstrained* learning objective to minimize the KL divergence between the class prior and the model-based conditional distribution, and solved it by EM algorithm, resulting in a procedure iterating between estimating the prior distribution and training the model.

Jin & Ghahramani (2003) used the class prior as the fitting target of the model, in which the label with maximum prior probability can be naturally regarded as the "true label". Coincidentally, the true label of training instance in PLL is obscured by candidate labels that hinder the learning. The key to success is also identifying the true label. Therefore, the foundational work enlightened the successors to identify the true label reasonably. Along this line, great efforts have been made in designing learning objectives with some elaborate *constraints* for making assumptions on the model (Chen et al., 2013; 2014) or better leveraging the prior knowledge (Nguyen & Caruana, 2008; Zhang & Yu, 2015; Yu & Zhang, 2017; Gong et al., 2017; Feng & An, 2019a) so as to recover the true labeling information.

However, the constrained learning objectives of the existing methods are coupled to some specific optimization algorithms. A non-linear time complexity in the total volume of data becomes a major limiting factor when these methods envision large amounts of training data. Furthermore, Bottou & Bousquet (2007) proved *stochastic optimization*,

[†]Preliminary work was done during an internship at RIKEN AIP. [1]School of Computer Science and Engineering, Southeast University, Nanjing, China [2]RIKEN Center for Advanced Intelligence Project, Tokyo, Japan [3]The University of Queensland, Australia [4]School of Computer Science and Engineering, Nanyang Technological University, Singapore [5]University of Tokyo, Tokyo, Japan. Correspondence to: Xin Geng <xgeng@seu.edu.cn>.

Proceedings of the 37^{th} International Conference on Machine Learning, Online, PMLR 119, 2020. Copyright 2020 by the author(s).

which few of the existing methods are compatible with, is the best choice for large-scale learning problems considering the estimation-optimization tradeoff. Therefore, the PLL problem is still practically challenging in *scaling up to big data*. In order to magnify PLL's potential on big data, we rethink critically whether the original unconstrained method in Jin & Ghahramani (2003) should be discarded, or is worth further studying in the deep learning era?

Our answer is in two folds. First, the decade-old method restricted to a simple linear model fed by the handcrafted features, which may be incompetent to represent and discriminate. Moreover, few PLL work hitherto can be generalized to deep network architectures. We would like to advance the previous work to enjoy the leading-edge models and optimizers from deep learning communities (Goodfellow et al., 2016). Second, the essence of our investigation is an algorithm agnostic in classification models. Thus we focus on a method that does not benefit purely from the network architecture, but also an innovative algorithm design.

In this paper, we aim at proposing a method of PLL with flexibility on the model and stochastic optimization. Towards this goal, we first derive a *classifier-consistent* risk estimator, and then propose a novel algorithm that is compatible with *arbitrary multi-class classifier* (ranging from linear to deep model) and stochastic optimizers. Experiments verify its superiority on synthetic and real-world partial-label datasets. Our contributions can be summarized as follows:

- Theoretically, we propose a classifier-consistent risk estimator for PLL, i.e., the classifier learned from partially labeled data converges to the optimal one learned from ordinarily labeled data under mild conditions. Then, we establish an estimation error bound for it.
- Practically, we propose a *progressive identification* method. The proposed method operates in a mini-batched training manner where the update of the model and the identification of true labels are accomplished seamlessly. This method is model-independent and loss-independent, as well as viable for any stochastic optimization (e.g., Robbins & Monro, 1951; Duchi et al., 2011).

2. Background

In this section, we formalize ordinary multi-class classification, partial-label learning, and complementary-label learning, and briefly review the related work.

2.1. Ordinary Multi-Class Classification

In ordinary multi-class classification, let $\mathcal{X} \subseteq \mathbb{R}^d$ be the instance space and $\mathcal{Y} = [c]$ be the label space, where d is the feature space dimension, $[c] := \{1, 2, \ldots, c\}$ and $c > 2$ is the number of classes. Let $p(x, y)$ be the underlying joint density of random variables $(X, Y) \in \mathcal{X} \times \mathcal{Y}$. The target is to learn a classifier $\boldsymbol{g} : \mathcal{X} \to \mathbb{R}^c$ that minimizes the estimator of the classification risk:

$$\mathcal{R}(\boldsymbol{g}) = \mathbb{E}_{(X,Y)\sim p(x,y)}[\ell(\boldsymbol{g}(X), \boldsymbol{e}^Y)], \tag{1}$$

in which $\ell : \mathbb{R}^c \times \boldsymbol{e}^{\mathcal{Y}} \to \mathbb{R}$ is a proper loss, i.e., it is continuous non-negative and $\ell(\hat{\eta}, \eta) = 0$ only when $\hat{\eta} = \eta$. $\boldsymbol{e}^{\mathcal{Y}} = \{\boldsymbol{e}^i : i \in \mathcal{Y}\}$ denotes the standard canonical vector in $\mathbb{R}^c$, i.e., the i-element in $\boldsymbol{e}^i$ equals 1 and others equal 0. Typically, the predicted label $\widehat{Y}$ is assumed to take the following form:

$$\widehat{Y} = \arg\max_{i\in\mathcal{Y}} g_i(X),$$

where $g_k(\cdot)$ is the k-th element of $\boldsymbol{g}(\cdot)$ that is interpreted as an estimate of the true label probability, i.e., $g_k(X) = p(Y = k|X)$. The hypothesis in $\mathcal{G}$ with minimal error $\boldsymbol{g}^* = \arg\min_{\boldsymbol{g}\in\mathcal{G}} \mathcal{R}(\boldsymbol{g})$ is the ordinary optimal classifier. We say a method is classifier-consistent if the learned classifier by the method converges to $\boldsymbol{g}^*$ by increasing the example size (Patrini et al., 2017; Xia et al., 2019).

Since $p(x, y)$ is usually unknown, the expectation in Eq. (1) is typically approximated by the average over the training examples $\{(x_i, y_i)\}_{i=1}^n \overset{\text{i.i.d.}}{\sim} p(x, y)$: $\widehat{\mathcal{R}}(\boldsymbol{g}) = \frac{1}{n}\sum_{i=1}^n [\ell(\boldsymbol{g}(x_i), \boldsymbol{e}^{y_i})]$, and $\widehat{\boldsymbol{g}} = \arg\min_{\boldsymbol{g}\in\mathcal{G}} \widehat{\mathcal{R}}(\boldsymbol{g})$ is returned by the empirical risk minimization (ERM) principle (Vapnik, 1998).

2.2. Partial-Label Learning

Different from ordinary multi-class classification, in PLL, the labelling information is weakened into candidate label set $S \in \mathcal{S}$, where $\mathcal{S} = \{\mathcal{P}(\mathcal{Y})/\emptyset/\mathcal{Y}\}$ is the power set of $\mathcal{Y}$ except for the empty set and the whole label set. Hence we need to train a classifier with access only to the partially labeled examples (X, S) drawn from the distribution with probability density $p(x, s)$, which is a marginal density of the complete density $p(x, y, s)$. Note that $p(x, y, s)$ can be decomposed into $p(x, s)$ and the class-probability density $p(y|x, s)$, or equivalently into the marginal density $p(x, y)$ and the class-conditional density $p(s|x, y)$. Then the basic definition for PLL that the true label Y of an instance X must be in its candidate label set S can be formulated as

$$\Pr_{(X,Y)\sim p(x,y), S\sim p(s|x,y)}(Y \in S) = 1. \tag{2}$$

The PLL risk estimator is defined over $p(x, s)$:

$$\mathcal{R}_{\mathrm{PLL}}(\boldsymbol{g}) = \mathbb{E}_{(X,S)\sim p(x,s)}[\ell_{\mathrm{PLL}}(\boldsymbol{g}(X), S)], \tag{3}$$

where $\ell_{\mathrm{PLL}} : \mathbb{R}^c \times \mathcal{P}(\mathcal{Y}) \to \mathbb{R}$. The goal of PLL is still inducing a multi-class classifier to assign the true labels for the unseen instances.

To estimate the risk in partially labeled data, defining ℓ_{PLL} matters. Jin & Ghahramani (2003) defined

$\ell_{\mathrm{PLL}}(\boldsymbol{g}(X), S) = \mathrm{KL}\big[\widehat{\boldsymbol{p}}(y|X)||\boldsymbol{g}(X)\big]$, in which $\widehat{\boldsymbol{p}}(y|X)$ represents the unknown prior distribution, and iteratively solved it. Following Jin & Ghahramani (2003), many *EM-based* methods have proposed. They added some constraints to the optimization objective for better leveraging implicit information over feature space and label space, and disambiguated candidate labels via iterative refining procedure. Chen et al. (2013; 2014) proposed methods based on dictionary learning, which seeked the sparsest dictionary mapping the feature to class prior, and then Shrivastava et al. (2015) extended the linear dictionary by the kernel trick. These methods were optimized by K-SVD algorithm (Aharon et al., 2006). Feng & An (2019a) formulated a convex-concave problem and proved its optimization is equivalent to a set of QP problems. Feng & An (2019b) also formulated a QP problem to enlarge the gap of label priors between two instances with completely different candidate labels. In addition, some *SVM-based* methods with the maximum margin constraints (Nguyen & Caruana, 2008; Yu & Zhang, 2017) that were solved by the off-the-shelf implementation on multi-class SVM (Fan et al., 2008), and a few *non-parametric* methods (Hullermeier & Beringer, 2006; Zhang & Yu, 2015; Gong et al., 2017) were proposed.

These methods were solved in specific low-efficient manners and incompatible with high-efficient stochastic optimization. Thus they could hardly handle large-scale datasets. To the best of our knowledge, only the latest work (Yao et al., 2020a;b) used DNNs with stochastic optimizers as the backbone of their algorithms, however, they restricted the networks to some specific architectures while our method is flexible on the learning models, and they also lacked a theoretical understanding of their methods.

2.3. Complementary-Label Learning

Complementary-label learning (CLL) (Ishida et al., 2017; Yu et al., 2018; Ishida et al., 2019) uses the supervised information specifying a class that an example does *not* belong to, and hence it can be considered as an extreme PLL case with $c-1$ candidate labels. Restricting each instance to associate with a single complementary label limits its potential because the labelers can easily annotate multiple candidate labels or complementary labels. Recently, Feng et al. (2020) proposed to learn with multiple complementary labels. Nonetheless, they proposed an explicit data generation process, while our work has no special requirement on this aspect. Empirical studies also show that our proposed method can achieve promising performance in different partial types (e.g. binomial or pair in Section 5).

3. Learning with Partial Labels

In this section, we define a classifier-consistent risk estimator, and theoretically establish an estimation error bound.

3.1. Classifier-Consistent Risk Estimator

To make Eq. (3) estimable, an intuitive way is through a surrogate loss that treats all the candidate labels equally (Jin & Ghahramani, 2003): $\ell_{\mathrm{PLL}}(\boldsymbol{g}(X), S) = 1/|S| \sum_{i\in S} \ell(\boldsymbol{g}(X), \boldsymbol{e}^i)$. Nonethelss, the true label may be overwhelmed by the distractive outputs of the multiple false positive labels. Therefore, we consider that only the true label contributes to retrieving the classifier. Capturing this idea we define the PLL loss as the *minimal loss* over the candidate label set:

$$\ell_{\mathrm{PLL}}(\boldsymbol{g}(X), S) = \min_{i\in S} \ell(\boldsymbol{g}(X), \boldsymbol{e}^i), \tag{4}$$

which immediately leads to a new risk estimator:

$$\mathcal{R}_{\mathrm{PLL}}(\boldsymbol{g}) = \mathbb{E}_{(X,S)\sim p(x,s)} \min_{i\in S} \ell(\boldsymbol{g}(X), \boldsymbol{e}^i). \tag{5}$$

For a detailed description of Eq. (4), we can disassemble it by defining a function in terms of Y as a classifier $\boldsymbol{g}$'s best guess at the true label:

$$Y^{\boldsymbol{g}} = \arg\min_{i\in S} \ell(\boldsymbol{g}(X), \boldsymbol{e}^i). \tag{6}$$

Then correspondingly the PLL loss can be rewritten into an equivalent expression, i.e., $\boldsymbol{g}$ only needs to fit the best guess $Y^{\boldsymbol{g}}$ among S:

$$\ell_{\mathrm{PLL}}(\boldsymbol{g}(X), S) = \min_{i\in S} \ell(\boldsymbol{g}(X), \boldsymbol{e}^i) = \ell(\boldsymbol{g}(X), \boldsymbol{e}^{Y^{\boldsymbol{g}}}).$$

From now on, we explain under which conditions Eq. (5) is classifier-consistent. We start investigating this question from the following two lemmas.

Lemma 1. *(Summarized from Sec.3.1 of Liu & Dietterich, 2014) The ambiguity degree is defined as*

$$\gamma = sup_{(X,Y)\sim p(x,y), \bar{Y}\in\mathcal{Y}, S\sim p(s|x,y), \bar{Y}\neq Y} \Pr(\bar{Y} \in S).$$

If $\gamma < 1$, i.e. under the small ambiguity degree condition, the PLL problem is ERM learnability.

γ is the maximum probability of a negative label $\bar{Y}$ co-occurs with the true label Y. The small ambiguity degree condition implies that except for the true label, no other labels will be one hundred percent included in the candidate label set, which guarantees a classification error made on any instance will be detected with probability at least $1-\gamma$.

Then we provide a condition of the identifiability of the ordinary optimal classifier.

Lemma 2. *(Yu et al., 2018) If ℓ is the cross-entropy loss or mean squared error loss, the optimal classifier $\boldsymbol{g}^*$ of Eq. (1) satisfies $g_i^*(X) = p(Y=i|X)$.*

With the above lemmas, we can prove Eq. (5) possess classifier-consistency under a reasonable assumption, that is, learning is conducted under the deterministic case.

Theorem 1. *Under the deterministic scenario, if the small ambiguity degree condition is satisfied, and cross-entropy or mean squared error loss is used, then, the PLL optimal classifier $\boldsymbol{g}^*_{\mathrm{PLL}}$ of Eq. (5) is equivalent to the ordinary optimal classifier $\boldsymbol{g}^*$ of Eq. (1), i.e., $\boldsymbol{g}^*_{\mathrm{PLL}} = \boldsymbol{g}^*$.*

It is natural to assume a deterministic learning scenario, i.e., the true label Y_X of an instance X is uniquely determined by the measurable function $\boldsymbol{g}^{**} : p(Y = i|X) = g_i^{**}(X), Y_X = \arg\max_{i\in\mathcal{Y}} g_i^{**}(X)$, for ensuring the basic definition for PLL, i.e., Eq. (2) always holds. In the light of Lemma 2, $\boldsymbol{g}^* = \boldsymbol{g}^{**}$. In this case, the optimal classifier $\boldsymbol{g}^*$ can be recovered by minimizing Eq. (5). The proof is provided in Appendix.

3.2. Estimation Error Bound

Let $\widehat{\mathcal{R}}_{\mathrm{PLL}}$ be the empirical counterpart of $\mathcal{R}_{\mathrm{PLL}}$, and $\widehat{\boldsymbol{g}}_{\mathrm{PLL}} = \arg\min_{\boldsymbol{g}\in\mathcal{G}} \widehat{\mathcal{R}}_{\mathrm{PLL}}(\boldsymbol{g})$ be the empirical risk classifier. Suppose $\mathcal{G}_y$ be a class of real functions, and $\mathcal{G} = \oplus_{y\in[c]}\mathcal{G}_y$ be a c-valued function class. Assume there is $C_{\boldsymbol{g}} > 0$ such that $\sup_{\boldsymbol{g}\in\mathcal{G}} ||\boldsymbol{g}||_\infty \leq C_{\boldsymbol{g}}$, and the loss function $\ell(\boldsymbol{g}(X), Y)$ is Lipschitz continuous for all $|\boldsymbol{g}| \leq C_{\boldsymbol{g}}$ with a Lipschitz constant L_ℓ and upper-bounded by M, i.e., $M = \sup_{X\in\mathcal{X},|\boldsymbol{g}|\leq C_{\boldsymbol{g}},Y\in\mathcal{Y}} \ell(\boldsymbol{g}(X), Y)$. The *Rademacher complexity* of $\mathcal{G}$ over $p(x)$ with sample size n is defined as $\mathfrak{R}_n(\mathcal{G})$ (Bartlett & Mendelson, 2002). Then we have the following estimation error bound.

Theorem 2. *For any $\delta > 0$, we have with probability at least $1 - \delta$,*

$$\mathcal{R}_{\mathrm{PLL}}(\widehat{\boldsymbol{g}}_{\mathrm{PLL}}) - \mathcal{R}_{\mathrm{PLL}}(\boldsymbol{g}^*_{\mathrm{PLL}}) \leq 4\sqrt{2}cL_\ell \sum_{y=1}^{c} \mathfrak{R}_n(\mathcal{G}_y) + 2M\sqrt{\frac{\log(2/\delta)}{2n}}. \tag{7}$$

The proof is given in Appendix. As $n \to \infty$, $\mathfrak{R}_n(\mathcal{G}_y) \to 0$ for all parametric models with a bounded norm. Hence, $\mathcal{R}_{\mathrm{PLL}}(\widehat{\boldsymbol{g}}_{\mathrm{PLL}}) \to \mathcal{R}_{\mathrm{PLL}}(\boldsymbol{g}^*_{\mathrm{PLL}})$ as the number of training data approaches infinity.

4. Benchmark Solution

In the previous section, based on a novel PLL loss Eq. (4) we provided a risk estimator Eq. (5) with intriguing theoretical properties. Although the estimator is without any assumption on the model used, the $\min$ operator makes optimization difficult, because if a wrong label i in Eq. (5) is selected in the beginning, the optimization will focus on the wrong label till the end. Thus we design a benchmark solution to approximately solve Eq. (5) according to the idea behind Eq. (4) that only one (true) label should be taken into account, and consequently we can easily implement the algorithm over arbitrary multi-class classifier and powerful stochastic optimization.

Algorithm 1 PRODEN Algorithm

input $\mathcal{D}$: the partial-label training set $\{(x_i, s_i)\}_{i=1}^n$,
T: number of epochs;
output Θ: model parameter for $\boldsymbol{g}(x;\Theta)$

Let $\mathcal{A}$ be an stochastic optimization algorithm;
Initialize uniform weights $\mathbf{w}^0$ according to Eq. (9);
for $t = 1$ to T **do**
  Shuffle training set $\mathcal{D}$ into B mini-batches;
  for $k = 1$ to B **do**
    Compute L according to Eq. (8);
    Set gradient $-\nabla_\Theta L$;
    Update $\mathbf{w}$ according to Eq. (10);
    Update Θ by $\mathcal{A}$;
  end for
end for

Specifically, we relax the $\min$ operator in Eq. (4) by the dynamic weights. In the first place, we require that ℓ can be decomposed into each label, i.e.,

$$\ell(\boldsymbol{g}(X), \boldsymbol{e}^Y) = \sum_{i=1}^{c} \ell(g_i(X), e_i^Y),$$

where e_i^Y is the i-th element of $\boldsymbol{e}^Y$. Many commonly used multi-class loss functions are decomposable, for example, ℓ can be the cross-entropy loss: $\ell_{\mathrm{CE}}(\boldsymbol{g}(X), \boldsymbol{e}^Y) = -\sum_{i=1}^c e_i^Y \log(g_i(X))$ or mean squared error loss: $\ell_{\mathrm{MSE}}(\boldsymbol{g}(X), \boldsymbol{e}^Y) = \sum_{i=1}^c (g_i(X) - e_i^Y)^2$. In this case, the empirical risk estimator is rewritten as follows:

$$\widehat{\mathcal{R}}_{\mathrm{PLL}} = \frac{1}{n}\sum_{i=1}^{n}\sum_{j=1}^{c} \mathrm{w}_{ij}\ell(g_j(x_i), e_j^{s_i}), \tag{8}$$

where $e_j^{s_i}$ is the j-th coordinate of $\boldsymbol{e}^{s_i}$ and $\boldsymbol{e}^{s_i} = \sum_{k\in s_i} \boldsymbol{e}^k$. $\mathbf{w}_i \in \Delta^{c-1}$ is the c-dimensional simplex and the j-th element of it, i.e., w_{ij}, is the corresponding label weight, i.e., the confidence of the j-th label being the true label of the i-th instance. With appropriate weights, i.e., $\mathrm{w}_{ij} = 1$ if $\arg\min_{k\in s_i} \ell(\boldsymbol{g}(x_i), \boldsymbol{e}^k) = j$ and 0 otherwise, which is in consonance with Eq. (6), Eq. (8) is equivalent to the empirical counterpart of Eq. (5). Ideally, the label with weight 1 is exactly the true label, i.e, j is the true label of x_i if $\mathrm{w}_{ij} = 1$, which means we have identified the true label successfully. To eventually achieve such an ideal situation, we propose an effective algorithm named *PRODEN* (*PRO*gressive i*DEN*tification).

Because the weights are latent, the minimizer of Eq. (8) cannot be solved directly. Inspiring by the EM algorithm,

we start by training an initial model with uniform weights:

$$\mathrm{w}_{ij} = \begin{cases} 1/|s_i| & \text{if } j \in s_i, \\ 0 & \text{otherwise.} \end{cases} \tag{9}$$

Thanks to the memorization effects (Arpit et al., 2017; Han et al., 2018), the networks will remember "frequent patterns" in the first few iterations. If the small ambiguity degree condition is satisfied, they tend to remember the true labels in the initial epochs, which guides us towards a discriminative classifier giving relatively low losses for more possible true labels. Next, the problem becomes how to retain the informative predictions and gradually filter out the false positive labels. Instead of estimating the weights in a separate E-step, we tackle it simply using the current predictions for slightly putting more weights on more possible labels:

$$\mathrm{w}_{ij} = \begin{cases} g_j(\boldsymbol{x}_i) \Big/ \sum_{k \in s_i} g_k(\boldsymbol{x}_i) & \text{if } \ j \in s_i, \\ 0 & \text{otherwise.} \end{cases} \tag{10}$$

In this fashion, the true labels are *progressively* identified, and the refined labels in turn help to improve the classifier. The overall procedure is summarized in Algorithm 1, whose identification step (Step 8) and optimization step (Step 9) are conducted in a *seamless* manner. Next we provide more detailed arguments about the superiority and generalization of the proposed method.

Firstly, PRODEN gets rid of the overfitting issues of EM methods. The previous *iterative* EM methods (Jin & Ghahramani, 2003; Tang & Zhang, 2017; Feng & An, 2019a) trained the model until convergence in the M-step, but overemphasizing the convergence may result in redundant computation and overfitting issues, as the model will eventually fit the initial inexact prior knowledge and make a less informative estimate in the E-step on which the subsequent learning is based. To mitigate these problems, our method advances the procedure by merging the E-step and M-step. Since the learning process has no clear separation of the E-step and M-step, the weights can be updated at any epoch such that the local convergence within each epoch is not necessary in our training process.

Secondly, PRODEN has great flexibility for models and loss functions. In the deep learning era, loss functions with different theoretical results are one of the key factors that affect the performance of DNNs (Ghosh et al., 2017). In this way, models are welcomed to be loss-independent that allows flexibility with any loss function (Ishida et al., 2019). However, existing PLL methods were restricted to some specific loss functions for optimizable, e.g., Jin & Ghahramani (2003) limited the loss function to the KL divergence; the loss function of Yao et al. (2020b) was a combination of multiple cross-entropy losses. Instead, our proposal is flexible enough to be compatible with a large group of decomposable losses. Moreover, we will show in Appendix that the proposed method is provably a generalization of Jin & Ghahramani (2003).

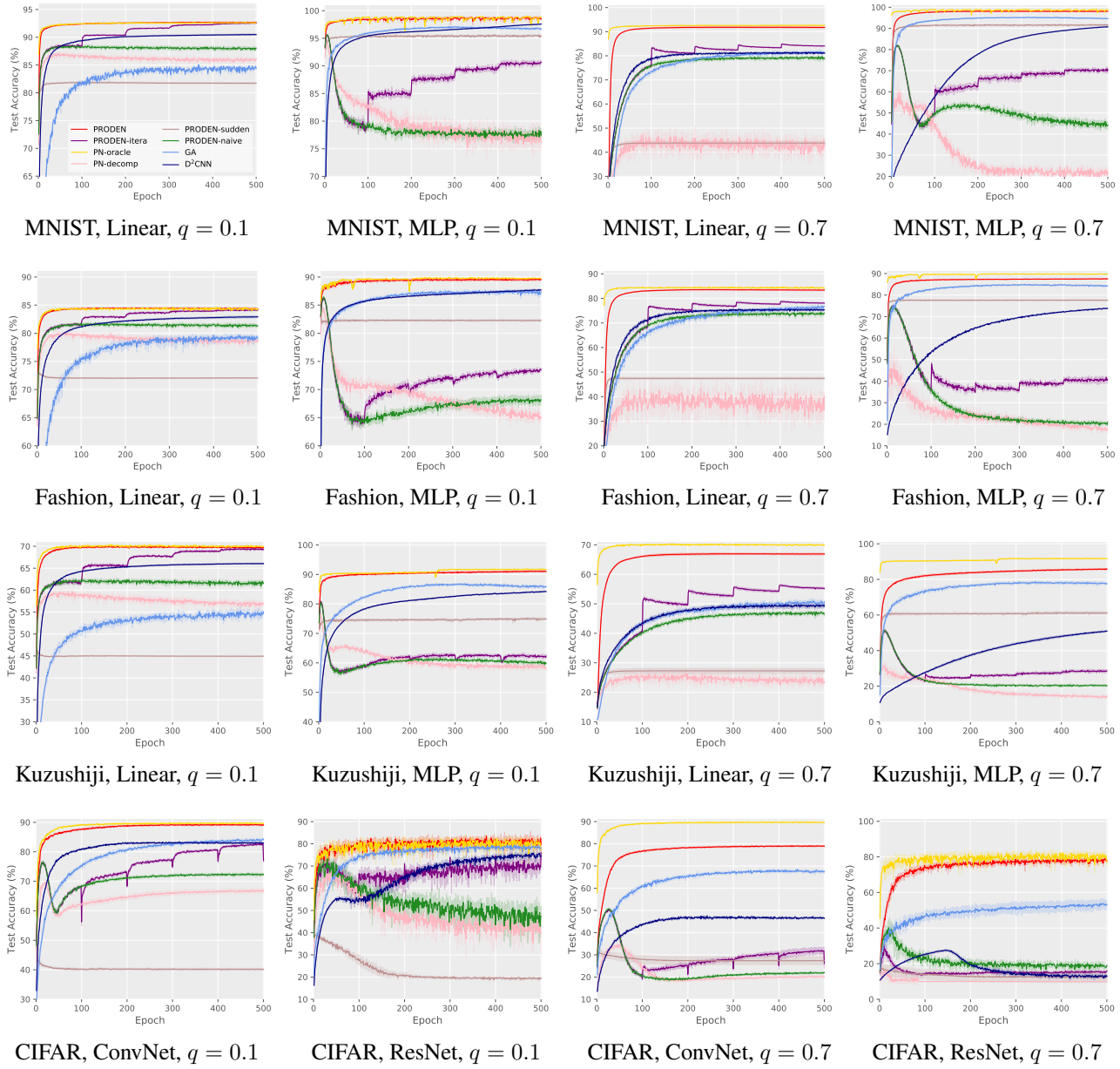
5. Experiments

In this section, we experimentally analyze the proposed method PRODEN, and compare with state-of-the-art PLL methods. The implementation is based on PyTorch (Paszke et al., 2019) and experiments were carried out with NVIDIA Tesla V100 GPU; it is available at `https://github.com/Lvcrezia77/PRODEN`.

Datasets We use four widely used benchmark datasets including MNIST (LeCun et al., 1998), Fashion-MNIST (H. Xiao & Vollgraf, 2017), Kuzushiji-MNIST (Clanuwat et al., 2018), and CIFAR-10 (Krizhevsky & Hinton, 2009), and five datasets from the UCI Machine Learning Repository (Krizhevsky & Hinton, 2009), including Yeast, Texture, Dermatology, Synthetic Control, and 20Newgroups. Similar to the corrupted strategy in label noise (Patrini et al., 2017; Han et al., 2018), we manually corrupt these datasets into partially labeled versions by a flipping probability q where $q = \Pr(\tilde{y} = 1 | y = 0)$ gives the probability that false positive label $\tilde{y}$ is flipped from negative label y. We adopt a *binomial* flipping strategy: $c - 1$ independent experiments are conducted on all training examples, each determining whether a negative label is flipped with probability q. Then for the examples that none of the negative labels is flipped, we additionally flip a random negative label to the candidate label set for ensuring all the training examples are partially labeled. In this paper, we conduct the experiments under both less-partial circumstances $q = 0.1$ and strong-partial circumstances $q = 0.7$. In addition, five real-world partial-label datasets are adopted, including Lost (Cour et al., 2011), Birdsong (Briggs et al., 2012), MSRCv2 (Liu & Dietterich, 2012), Soccer Player (Zeng et al., 2013), and Yahoo! News (Guillaumin et al., 2010).

Baselines We first analyze PRODEN by comparing it with seven baseline methods based on DNNs, including three variants of PRODEN, two supervised methods, and two state-of-the-art PLL methods:

- *PRODEN-itera* means updating the label weights in the iterative EM manner instead of a seamless manner proposed in Section 4.
- *PRODEN-sudden* means performing a *sudden* identification, i.e., updating the weights $w_{ik} = 1$ if $\arg\max_{j \in s_i} g_j(x_i) = k$ and $w_{ij} = 0, \forall j \neq k$ in every iteration step.
- *PRODEN-naive* means never updating the uniform weights.
- *PN-oracle* means supervised learning from ordinary labels. It should achieve the best performance, and is used merely for a proof of concept.



MNIST, Linear, $q = 0.1$ | MNIST, MLP, $q = 0.1$ | MNIST, Linear, $q = 0.7$ | MNIST, MLP, $q = 0.7$

Fashion, Linear, $q = 0.1$ | Fashion, MLP, $q = 0.1$ | Fashion, Linear, $q = 0.7$ | Fashion, MLP, $q = 0.7$

Kuzushiji, Linear, $q = 0.1$ | Kuzushiji, MLP, $q = 0.1$ | Kuzushiji, Linear, $q = 0.7$ | Kuzushiji, MLP, $q = 0.7$

CIFAR, ConvNet, $q = 0.1$ | CIFAR, ResNet, $q = 0.1$ | CIFAR, ConvNet, $q = 0.7$ | CIFAR, ResNet, $q = 0.7$

Figure 1. Test accuracy for various models and datasets. Dark colors show the mean accuracy of 5 trials and light colors show standard deviation. Fashion is short for Fashion-MNIST, Kuzushiji is short of Kuzushiji-MNIST, CIFAR is short of CIFAR-10.

- *PN-decomp* means decomposing one instance with multiple candidate labels into many (same) instances each one single label, so that we could use any ordinary multi-class classification methods.
- *D^2CNN* (Yao et al., 2020b) means a PLL learning method based on DNNs.
- *GA* (Ishida et al., 2019) means a CLL method based on DNNs and gradient ascent.

We employ multiple base models, including linear model, 5-layer perceptron (MLP), 12-layer ConvNet (Laine & Aila, 2017) and 32-layer ResNet (He et al., 2016) to show that our proposal is compatible with a wide family of learning models. The detailed descriptions of the datasets with their corresponding models are provided in Appendix. The optimizer is stochastic gradient descent (SGD) (Robbins & Monro, 1951) with momentum 0.9. We train each model 500 epochs with softmax function and cross-entropy loss. And PRODEN-itera updates label weights every 100 epochs.

We further compare PRODEN with six classical PLL methods that can hardly be implemented by DNNs on small-scale

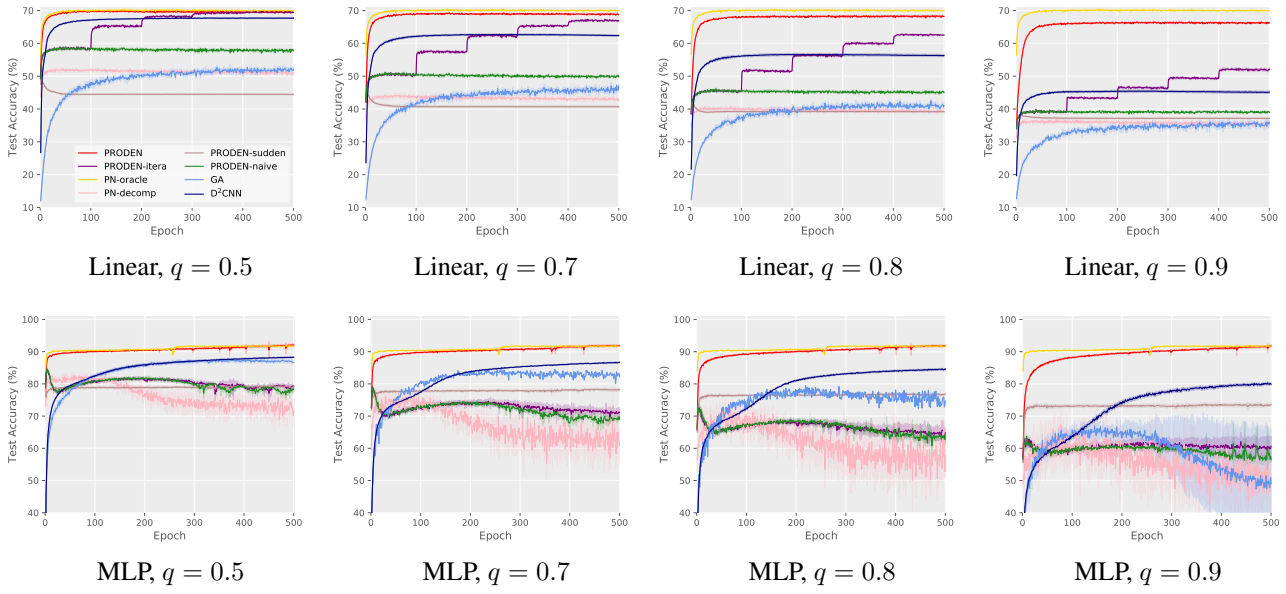


Figure 2. Test accuracy on Kuzushiji-MNIST in the pair case.

datasets (UCI and real-world datasets). They are four parametric methods: *SURE* (Feng & An, 2019a), *CLPL* (Cour et al., 2011), *ECOC* (Zhang et al., 2017), *PLSVM* (Nguyen & Caruana, 2008), and two non-parametric methods: *PLkNN* (Hullermeier & Beringer, 2006) and *IPAL* (Zhang & Yu, 2015). Their hyper-parameters are selected according to the suggested parameter settings in original papers. Detailed information is provided in Appendix. For a fair comparison, PRODEN and all the parametric methods employ a linear model. We average the classification accuracy of PRODEN over the last 10 epochs as the results to prove that PRODEN is always stable and will not cause performance degradation due to overfitting when the number of epochs increases.

Results on benchmark datasets We record inductive results which indicate the classification accuracy in the test set (test accuracy). The means and standard deviations of test accuracy based on 5 random samplings in the binomial case are shown in Figure 1. The transductive accuracy which reflects the ability in identifying the true labels in the training set can be found in Appendix.

We first observe the performance when $q = 0.1$ (the left two columns). PRODEN is always the best method and comparable to PN-oracle with all the models. PRODEN-itera is comparable to PRODEN with a linear model, but its performance deteriorates drastically with complex models because of the overfitting issues. This phenomenon is consistent with the discussions in Section 4. In PRODEN-naive, the weights are always equally distributed, while in PRODEN-sudden, the sudden identification concentrates all the weights to the winners, resulting in their poorer performance.

Next, we compare these methods when $q = 0.7$ (the right two columns). This is significantly harder than $q = 0.1$. But when the task difficulty is relatively low (e.g. MNIST, Fashion-MNIST), PRODEN is still comparable to PN-oracle with such a large flipping probability, while the performance of the baselines is greatly reduced. The superiority always stands out for PRODEN compared with two latest deep methods GA and D^{2}CNN.

Analysis on the ambiguity degree It is intuitive that the higher the ambiguity degree is, the more difficult it is to find the true labels. We investigate the influence of ambiguity degree γ through a *pair* flipping strategy: only the classes that are similar to the true class will be put into the candidate label set with probability q. We gradually move q from 0.5 to 0.9 to simulate γ ($\gamma \to q$ as $n \to \infty$), and the experimental results on Kuzushiji-MNIST are reported in Figure 2, and phenomena on other datasets are similar and reported in Appendix. We can see that even when the ambiguity degree is high, PRODEN is still highly competitive. PRODEN tends to be less affected with increased ambiguity, while the baselines are affected severely.

Results on small-scale datasets We perform five-fold cross-validation, and use paired t-test at 5% significance level. Table 1 and Table 2 report the mean test accuracy with standard deviation on UCI datasets and the real-world datasets, respectively. $\bullet/\circ$ represents whether PRODEN is significantly better/worse than the comparing methods. Clearly, PRODEN is overall the best performing, confirming the advantage of PRODEN afforded not only by the network architecture, but also the progressive identification process.

Table 1. Test accuracy (mean±std) on the UCI datasets in the binomial case.

	q	Yeast	Texture	Dermatology	Synthetic Control	20Newsgroups
PRODEN	0.1	**59.05±4.66%**	99.64±0.16%	**96.16±3.26%**	**98.33±1.32%**	77.28±0.68%
	0.7	**55.15±3.87%**	**99.33±0.32%**	**95.34±3.15%**	**95.00±4.75%**	**64.74±0.90%**
PRODEN-itera	0.1	57.55±3.96%	**99.73±0.13%**	95.56±2.90%	82.38±4.18%•	77.04±0.77%
	0.7	53.62±5.54%	94.79±1.63%•	76.22±4.48%•	48.33±7.96%•	52.43±0.75%•
GA	0.1	25.43±3.81%•	96.77±0.51%•	73.53±7.73%•	64.70±0.42%•	66.53±2.60%•
	0.7	22.59±2.51%•	95.76±0.62%•	52.00±12.32%•	49.72±6.38%•	56.47±0.59%•
D^2CNN	0.1	59.05±4.66%	98.80±0.31%•	95.34±2.29%	84.50±11.28%•	73.20±0.46%•
	0.7	55.15±3.87%	97.23±0.71%•	91.59±1.08%•	71.00±13.02%•	52.13±0.41%•
SURE	0.1	55.52±4.92%	97.96±0.32%•	95.16±2.25%	76.67±2.83%•	69.82±0.26%•
	0.7	49.32±3.95%•	94.75±3.68%•	90.96±2.02%•	54.67±7.67%•	62.66±1.21%•
CLPL	0.1	57.90±4.35%	98.78±0.22%•	94.79±3.27%	78.00±3.10%•	76.26±0.77%
	0.7	54.88±7.78%	95.09±1.01%•	92.33±2.67%•	63.33±7.02%•	50.37±0.57%•
ECOC	0.1	59.01±3.72%	99.15±0.27%•	94.71±2.08%	96.67±2.08%	**77.67±1.11%**
	0.7	53.37±2.37%•	97.69±0.82%•	91.47±3.02%•	91.67±2.08%•	61.32±2.45%•
PLSVM	0.1	54.73±2.89%	93.75±1.99%•	92.88±2.25%•	92.50±2.12%•	76.25±1.22%
	0.7	42.34±1.92%•	50.69±5.62%•	89.32±4.98%•	85.50±2.61%•	59.12±0.41%•
PLkNN	0.1	54.28±3.64%	97.20±0.28%•	94.52±2.74%	94.83±2.08%•	42.39±0.97%•
	0.7	28.72±1.01%•	96.78±0.31%•	85.48±3.70%•	85.50±6.36%•	18.01±0.34%•
IPAL	0.1	50.56±2.83%•	99.33±0.26%•	95.34±2.29%	98.33±0.83%	75.01±0.69%•
	0.7	41.10±3.71%•	97.84±0.57%•	95.02±2.03%	94.83±6.55%	56.93±0.50%•

Table 2. Test accuracy (mean±std) on the real-world datasets.

	Lost	Birdsong	MSRCv2	Soccer Player	Yahoo! News
PRODEN	**76.57±1.47%**	**72.01±0.44%**	45.27±1.73%	**55.99±0.58%**	**67.40±0.55%**
PRODEN-itera	68.09±3.78%•	68.02±0.76%•	42.79±2.80%	53.50±0.94%•	67.04±0.67%
D^2CNN	69.61±5.48%•	66.58±1.49%•	40.17±1.99%•	49.06±0.15%•	56.39±0.89%•
GA	48.21±4.44%•	29.77±1.43%•	22.30±2.71%•	51.88±0.44%•	34.32±0.95%•
SURE	71.61±3.44%•	58.04±1.22%•	31.57±2.48%•	49.16±0.20%•	45.73±0.90%•
CLPL	76.17±1.81%	67.56±1.12%•	43.64±0.24%	49.88±4.29%•	53.74±0.95%•
ECOC	63.93±5.45%•	71.47±1.24%•	46.78±2.84%	55.51±0.54%	64.78±0.78%•
PLSVM	72.86±5.45%•	60.46±1.99%•	38.97±4.62%•	46.15±1.00%•	60.46±1.48%•
PLkNN	35.00±4.71%•	64.22±1.14%•	41.60±2.30%•	49.18±0.26%•	40.30±0.90%•
IPAL	71.25±1.40%•	71.19±1.54%	**52.36±2.87%**○	54.41±0.56%•	66.22±0.80%•

6. Conclusion

In this paper, we focused on proposing a novel method for PLL which is compatible with flexible multi-class classifiers and stochastic optimization. We first proposed a classifier-consistent risk estimator based on the minimal loss incurred by candidate labels. The estimator has good theoretical properties, while the $\min$ operator makes it difficult to be solved by the epoch-wise optimization of neural networks. Therefore, we proposed a progressive identification method named PRODEN for approximately minimizing the proposed risk estimator, whose idea is relaxing $\min$ to a weighted combination. Learning the weights and the classifier are then conducted in a seamless manner for mitigating the overfitting problem. At last, experiments demonstrated that the proposed method could successfully train various models, and it compared favorably with state-of-the-art methods.

Acknowledgements

JL and XG were supported by the National Key Research & Development Plan of China (No. 2017YFB1002801), the National Science Foundation of China (61622203), the Collaborative Innovation Center of Novel Software Technology and Industrialization, and the Collaborative Innovation Center of Wireless Communications Technology. MX was supported by the Open Project Program of the State Key Lab. for Novel Software Technology, Nanjing University, Nanjing, 210093, P.R.China. LF was supported by MOE, NRF, and NTU, Singapore. GN and MS were supported by JST AIP Acceleration Research Grant Number JPMJCR20U3, Japan.

References

Aharon, M., Elad, M., and Bruckstein, A. M. The k-svd: An algorithm for designing of overcomplete dictionaries for sparse representation. *IEEE Transactions on Signal Processing*, 54(11):4311–4322, 2006.

Arpit, D., Jastrzebski, S., Ballas, N., Krueger, D., Bengio, E., Kanwal, M., Maharaj, T., and Fischer, A. A closer look at memorization in deep networks. In *Proceedings of 34th International Conference on Machine Learning (ICML'17)*, pp. 233–242, Sydney, Australia, 2017.

Bartlett, P. L. and Mendelson, S. Rademacher and gaussian complexities: Risk bounds and structural results. *Journal of Machine Learning Research*, 3(11):463–482, 2002.

Bertsekas, D. P. Nonlinear programming. *Journal of the Operational Research Society*, 48(3):334–334, 1997.

Bottou, L. and Bousquet, O. The tradeoffs of large scale learning. In *Advances in Neural Information Processing Systems 20 (NIPS'07)*, volume 20, pp. 1–8, Vancouver, Canada, 2007.

Briggs, F., Fern, X. Z., and Raich, R. Rank-loss support instance machines for miml instance annotation. In *Proceedings of the 18th ACM SIGKDD International Conference on Knowledge Discovery and Data Mining (KDD'12)*, pp. 534–542, Beijing, China, 2012.

Chen, C., Patel, V. M., and Chellappa, R. Learning from ambiguously labeled face images. *IEEE Transactions on Pattern Analysis and Machine Intelligence*, 40(7):1653–1667, 2018.

Chen, Y., Patel, V. M., Pillai, J. K., Chellappa, R., and Phillips, P. J. Dictionary learning from ambiguously labeled data. In *Proceedings of the 26th IEEE Conference on Computer Vision and Pattern Recognition (CVPR'13)*, pp. 353–360, Portland, OR, 2013.

Chen, Y., Patel, V. M., Pillai, J. K., Chellappa, R., and Phillips, P. J. Ambiguously labeled learning using dictionaries. *IEEE Transactions on Information Forensics and Security*, 9(12):2076–2088, 2014.

Clanuwat, T., Bober-Irizar, M., Kitamoto, A., Lamb, A., Yamamoto, K., and Ha, D. Deep learning for classical japanese literature. *arXiv preprint arXiv:1812.01718*, 2018.

Cour, T., Sapp, B., and Taskar, B. Learning from partial labels. *Journal of Machine Learning Research*, 12(5): 1501–1536, 2011.

Duchi, J., Hazan, E., and Singer, Y. Adaptive subgradient methods for online learning and stochastic optimization. *Journal of Machine Learning Research*, 12(7):2121–2159, 2011.

Fan, R., Chang, K., Hsieh, C., Wang, X., and Lin, C. Liblinear: A library for large linear classification. *Journal of Machine Learning Research*, 9(8):1871–1874, 2008.

Feng, L. and An, B. Partial label learning with self-guided retraining. In *Proceedings of 33rd AAAI Conference on Artificial Intelligence (AAAI'19)*, pp. 3542–3549, Honolulu, HI, 2019a.

Feng, L. and An, B. Partial label learning by semantic difference maximization. In *Proceedings of the 28th International Joint Conference on Artificial Intelligence (IJCAI'19)*, pp. 2294–2300, Macao, China, 2019b.

Feng, L., Kaneko, T., Han, B., Niu, G., An, B., and Sugiyama, M. Learning with multiple complementary labels. In *Proceedings of 37th International Conference on Machine Learning (ICML'20)*, 2020.

Ghosh, A., Kumar, H., and Sastry, P. Robust loss functions under label noise for deep neural networks. In *Proceedings of 31st AAAI Conference on Artificial Intelligence (AAAI'17)*, pp. 1919–1925, San Francisco, CA, 2017.

Gong, C., Liu, T., Tang, Y., Yang, J., Yang, J., and Tao, D. A regularization approach for instance-based superset label learning. *IEEE Transactions on Cybernetics*, 48(3): 967–978, 2017.

Gong, C., Shi, H., Liu, T., Zhang, C., Yang, J., and Tao, D. Loss decomposition and centroid estimation for positive and unlabeled learning. *IEEE Transactions on Pattern Analysis and Machine Intelligence*, 2019.

Goodfellow, I., Bengio, Y., and Courville, A. *Deep Learning*. MIT Press, 2016.

Guillaumin, M., Verbeek, J., and Schmid, C. Multiple instance metric learning from automatically labeled bags

of faces. *Lecture Notes in Computer Science*, 63(11): 634–647, 2010.

H. Xiao, K. R. and Vollgraf, R. Fashion-mnist: a novel image dataset for benchmarking machine learning algorithms. *arXiv preprint arXiv:1708.07747*, 2017.

Han, B., Yao, Q., Yu, X., Niu, G., Xu, M., Hu, W., Tsang, I., and Sugiyama, M. Co-teaching: Robust training of deep neural networks with extremely noisy labels. In *Advances in Neural Information Processing Systems 31 (NeurIPS'18)*, pp. 8527–8537, Montreal, Canada, 2018.

He, K., Zhang, X., Ren, S., and Sun, J. Deep residual learning for image recognition. In *Proceedings of the 29th IEEE conference on Computer Vision and Pattern Recognition (CVPR'16)*, pp. 770–778, Las Vegas, NV, 2016.

Hullermeier, E. and Beringer, J. Learning from ambiguously labeled examples. *Intelligent Data Analysis*, 10(5):419–439, 2006.

Ioffe, S. and Szegedy, C. Batch normalization: Accelerating deep network training by reducing internal covariate shift. In *Proceedings of the 32nd International Conference on Machine Learning (ICML'15)*, pp. 448–456, Lille, France, 2015.

Ishida, T., Niu, G., Hu, W., and Sugiyama, M. Learning from complementary labels. In *Advances in Neural Information Processing Systems 30 (NIPS'17)*, pp. 5639–5649, Long Beach, CA, 2017.

Ishida, T., Niu, G., Menon, A. K., and Sugiyama, M. Complementary-label learning for arbitrary losses and models. In *Proceedings of 36th International Conference on Machine Learning (ICML'19)*, pp. 2971–2980, Long Beach, CA, 2019.

Jin, R. and Ghahramani, Z. Learning with multiple labels. In *Advances in Neural Information Processing Systems 16 (NIPS'03)*, pp. 921–928, Vancouver, Canada, 2003.

Kamnitsas, K., Castro, D. C., Folgoc, L. L., Walker, I., Tanno, R., Rueckert, D., Glocker, B., Criminisi, A., and Nori, A. Semi-supervised learning via compact latent space clustering. In *Proceedings of 35th International Conference on Machine Learning (ICML'18)*, pp. 2464–2473, Stockholm, Sweden, 2018.

Krizhevsky, A. and Hinton, G. Learning multiple layers of features from tiny images. 2009.

Laine, S. and Aila, T. Temporal ensembling for semi-supervised learning. In *Proceedings of 5th International Conference on Learning Representations (ICLR'17)*, Toulon, France, 2017.

LeCun, Y., Bottou, L., Bengio, Y., and Haffner, P. Gradient-based learning applied to document recognition. *Proceedings of the IEEE*, 86(11):2278–2324, 1998.

Ledoux, M. and Talagrand, M. *Probability in Banach Spaces: Isoperimetry and Processes*. Springer Science & Business Media, 2013.

Liu, L. and Dietterich, T. G. A conditional multinomial mixture model for superset label learning. In *Advances in Neural Information Processing Systems 25 (NIPS'12)*, pp. 548–556, Lake Tahoe, NV, 2012.

Liu, L. and Dietterich, T. G. Learnability of the superset label learning problem. In *Proceedings of 31st International Conference on Machine Learning (ICML'14)*, pp. 1629–1637, Beijing, China, 2014.

Lu, N., Niu, G., Menon, A. K., and Sugiyama, M. On the minimal supervision for training any binary classifier from only unlabeled data. In *Proceedings of 7th International Conference on Learning Representations (ICLR'19)*, New Orleans, LA, 2019.

Luo, J. and Orabona, F. Learning from candidate labeling sets. In *Advances in Neural Information Processing Systems 23 (NIPS'10)*, pp. 1504–1512, Vancouver, Canada, 2010.

Lyu, G., Feng, S., Wang, T., Lang, C., and Li, Y. Gm-pll: Graph matching based partial label learning. *IEEE Transactions on Knowledge and Data Engineering*, 2019.

Maas, A. L., Hannun, A. Y., and Ng, A. Y. Rectifier nonlinearities improve neural network acoustic models. In *Proceedings of 30th International Conference on Machine Learning (ICML'13)*, volume 30, pp. 3, Atlanta, GA, 2013.

Masnadi-Shirazi, H. and Vasconcelos, N. On the design of loss functions for classification: theory, robustness to outliers, and savageboost. In *Advances in Neural Information Processing Systems 22 (NIPS'09)*, pp. 1049–1056, Vancouver, Canada, 2009.

Maurer, A. A vector-contraction inequality for rademacher complexities. In *International Conference on Algorithmic Learning Theory (ALT'16)*, pp. 3–17, 2016.

McDiarmid, C. On the method of bounded differences. *Surveys in combinatorics*, 141(1):148–188, 1989.

Nguyen, N. and Caruana, R. Classification with partial labels. In *Proceedings of the 14th ACM SIGKDD International Conference on Knowledge Discovery and Data Mining (KDD'08)*, pp. 381–389, Las Vegas, NV, 2008.

Panis, G. and Lanitis, A. An overview of research activities in facial age estimation using the fg-net aging database. In *Proceedings of the 13th European Conference on Computer Vision (ECCV'14)*, pp. 737–750, Zurich, Switzerland, 2014.

Paszke, A., Gross, S., Massa, F., Lerer, A., Bradbury, J., Chanan, G., Killeen, T., Lin, Z., Gimelshein, N., Antiga, L., et al. Pytorch: An imperative style, high-performance deep learning library. In *Advances in Neural Information Processing Systems 32 (NeurIPS'19)*, pp. 8024–8035, Vancouver, Canada, 2019.

Patrini, G., Rozza, A., Menon, A. K., Nock, R., and Qu, L. Making deep neural networks robust to label noise: A loss correction approach. In *Proceedings of the 30th IEEE Conference on Computer Vision and Pattern Recognition (CVPR'17)*, pp. 1944–1952, Honolulu, HI, 2017.

Robbins, H. and Monro, S. A stochastic approximation method. *The Annals of Mathematical Statistics*, 22(3): 400–407, 1951.

Shrivastava, A., Patel, V. M., and Chellappa, R. Non-linear dictionary learning with partially labeled data. *Pattern Recognition*, 48(11):3283–3292, 2015.

Tang, C. and Zhang, M. Confidence-rated discriminative partial label learning. In *Proceedings of 31st AAAI Conference on Artificial Intelligence (AAAI'17)*, pp. 2611–2617, San Francisco, CA, 2017.

Vapnik, V. N. Statistical learning theory. *John Wiley & Sons*, 1998.

Wang, H., Liu, W., Zhao, Y., Zhang, C., Hu, T., and Chen, G. Discriminative and correlative partial multi-label learning. In *Proceedings of 28th International Joint Conference on Artificial Intelligence (IJCAI'19)*, pp. 3691–3697, Macao, China, 2019.

Xia, X., Liu, T., Wang, N., Han, B., Gong, C., Niu, G., and Sugiyama, M. Are anchor points really indispensable in label-noise learning? In *Advances in Neural Information Processing Systems 32 (NeurIPS'19)*, pp. 6838–6849, Vancouver, Canada, 2019.

Yao, Y., Chen, G., Deng, J., and Yang, J. Network cooperation with progressive disambiguation for partial label learning. *arXiv preprint arXiv:2002.11919*, 2020a.

Yao, Y., Gong, C., Deng, J., Chen, X., Wu, J., and Yang, J. Deep discriminative cnn with temporal ensembling for ambiguously-labeled image classification. In *Proceedings of 34th AAAI Conference on Artificial Intelligence (AAAI'20)*, New York, NY, in press, 2020b.

Yu, F. and Zhang, M. Maximum margin partial label learning. *Machine Learning*, 106(4):573–593, 2017.

Yu, X., Liu, T., Gong, M., and Tao, D. Learning with biased complementary labels. In *Proceedings of the 15th European Conference on Computer Vision (ECCV'18)*, pp. 68–83, Munich, Germany, 2018.

Zeng, Z., Xiao, S., Jia, K., Chan, T., Gao, S., Xu, D., and Ma, Y. Learning by associating ambiguously labeled images. In *Proceedings of the 26th IEEE Conference on Computer Vision and Pattern Recognition (CVPR'13)*, pp. 708–715, Portland, OR, 2013.

Zhang, M. and Yu, F. Solving the partial label learning problem: An instance-based approach. In *Proceedings of the 24th International Joint Conference on Artificial Intelligence (IJCAI'15)*, pp. 4048–4054, Buenos Aires, Argentina, 2015.

Zhang, M., Yu, F., and Tang, C. Disambiguation-free partial label learning. *IEEE Transactions on Knowledge and Data Engineering*, 29(10):2155–2167, 2017.

Zhou, Z. A brief introduction to weakly supervised learning. *National Science Review*, 5(1):44–53, 2017.

Supplementary Material

A. Proof of Lemma 2

Cross-Entropy loss According to (Masnadi-Shirazi & Vasconcelos, 2009), since the ℓ_{CE} is non-negative, minimizing the conditional risk $\mathbb{E}_{p(y|x)}[\ell_{\mathrm{CE}}(\boldsymbol{g}(X), Y)|X], \forall X \in \mathcal{X}$ is an alternative of minimizing $\mathcal{R}(\boldsymbol{g})$. The conditional risk can be written as

$$\mathcal{C}(\boldsymbol{g}) = -\sum_{i=1}^{c} p(Y=i|X)\log(g_i(X)), \quad \text{s.t.} \sum_{i=1}^{c} g_i(X) = 1.$$

By the Lagrange Multiplier method (Bertsekas, 1997), we have

$$\mathcal{L} = -\sum_{i=1}^{c} p(Y=i|X)\log(g_i(X)) + \lambda(\sum_{i=1}^{c} g_i(X) - 1).$$

To minimize $\mathcal{L}$, we take the partial derivative of $\mathcal{L}$ with respect to g_i and set it be 0:

$$g_i^*(X) = \frac{1}{\lambda} p(Y=i|X).$$

Because $\sum_{i=1}^{c} g_i^*(X) = 1$ and $\sum_{i=1}^{c} g_i^*(X) = 1$, we have

$$\sum_{i=1}^{c} g_i^*(X) = \frac{1}{\lambda}\sum_{i=1}^{c} p(Y=i|X) = 1.$$

Therefore, we can obtain $\lambda = 1$ that ensures $g_i^*(X) = p(Y=i|X), \forall i \in [c], \forall X \in \mathcal{X}$, which concludes the proof.

Mean squared error loss Analogously, if the mean squared error loss is used, we can write the optimization problem as

$$\mathcal{C}(\boldsymbol{g}) = \sum_{i=1}^{c}(p(Y=i|X) - g_i(X))^2, \quad \text{s.t.} \sum_{i=1}^{c} g_i(X) = 1.$$

By the Lagrange Multiplier method, we have

$$\mathcal{L} = \sum_{i=1}^{c}(p(Y=i|X) - g_i(X))^2 - \lambda'(\sum_{i=1}^{c} g_i(X) - 1).$$

By setting the derivative to 0, we obtain

$$g_i^*(X) = \frac{\lambda'}{2} + p(Y=i|X).$$

Because $\sum_{i=1}^{c} g_i^*(X) = 1$ and $\sum_{i=1}^{c} g_i^*(X) = 1$, we have

$$\sum_{i=1}^{c} g_i^*(X) = \frac{\lambda' c}{2} + \sum_{i=1}^{c} p(Y=i|X).$$

Since $c \neq 0$, we can obtain $\lambda' = 0$. In this way, $g_i^*(X) = p(Y=i|X), \forall i \in [c], \forall X \in \mathcal{X}$, which concludes the proof. □

B. Proof of Theorem 1

First we prove $\boldsymbol{g}^*$ is the optimal classifier for PLL by substituting the $\boldsymbol{g}^*$ into the PLL risk estimator Eq. (5):

$$\begin{aligned}
\mathcal{R}_{\mathrm{PLL}}(\boldsymbol{g}^*) &= \mathbb{E}_{(X,S)\sim p(x,s)} \min_{i\in S} \ell(\boldsymbol{g}^*(X), \boldsymbol{e}^i) = \int \sum_{S\in\mathcal{S}} \min_{i\in S} \ell(\boldsymbol{g}^*(X), \boldsymbol{e}^i) p(s|x)p(x)dX \\
&= \int \sum_{S\in\mathcal{S}} \min_{i\in S} \ell(\boldsymbol{g}^*(X), \boldsymbol{e}^i) \sum_{Y\in\mathcal{Y}} p(s,y|x)p(x)dX \\
&= \int \sum_{Y\in\mathcal{Y}} \sum_{S\in\mathcal{S}} \min_{i\in S} \ell(\boldsymbol{g}^*(X), \boldsymbol{e}^i) p(s|x,y)p(y|x)p(x)dX \\
&= \int \sum_{Y\in\mathcal{Y}} \sum_{S\in\mathcal{S}} \ell(\boldsymbol{g}^*(X), \boldsymbol{e}^{Y_X}) p(s|x,y)p(y|x)p(x)dX \\
&= \int \sum_{Y\in\mathcal{Y}} \ell(\boldsymbol{g}^*(X), \boldsymbol{e}^{Y_X}) \sum_{S\in\mathcal{S}} p(s|x,y)p(y|x)p(x)dX \\
&= \int \sum_{Y\in\mathcal{Y}} \ell(\boldsymbol{g}^*(X), \boldsymbol{e}^{Y_X}) p(x,y)dX = \mathcal{R}(\boldsymbol{g}^*) = 0.
\end{aligned}$$

where we have used $\min_{i\in S} \ell(\boldsymbol{g}^*(X), \boldsymbol{e}^i) = \ell(\boldsymbol{g}^*(X), \boldsymbol{e}^{Y_X})$ because ℓ is a proper loss and the derministic assumption is made. This indicates that the PLL risk has been minimized by $\boldsymbol{g}^*$.

On the other hand, we prove $\boldsymbol{g}^*$ is the only solution to Eq. (5) by contradiction, namely, there is at least one other solution $\boldsymbol{h}$ enables $\mathcal{R}_{\mathrm{PLL}}(\boldsymbol{h}) = 0$, and predicts different label $Y^{\boldsymbol{h}} \neq Y_X$ for at least one instance X. Hence for any $S \ni Y_X$ we have

$$\min_{i\in S} \ell(\boldsymbol{h}(X), \boldsymbol{e}^i) = \ell(\boldsymbol{h}(X), \boldsymbol{e}^{Y^{\boldsymbol{h}}}) = 0.$$

Nevertheless, the above equality is always true unless $Y^{\boldsymbol{h}}$ is invariably included in the candidate label set of X, i.e., $\Pr_{S\sim p(s|x,y)}(Y^{\boldsymbol{h}} \in S) = 1$. Obviously, this contradicts the small ambiguity degree condition. Therefore, there is one, and only one minimizer of the PLL risk estimator, which is the same as the minimizer learned from ordinarily labeled data. The proof is complete. □

C. Proof of Theorem 2

First, we show the uniform deviation bound, which is useful to derive the estimation error bound.

Lemma 3. *For any $\delta > 0$, we have with probability at least $1-\delta$,*

$$\sup_{\boldsymbol{g}\in\mathcal{G}} \left| \mathcal{R}_{\mathrm{PLL}}(\boldsymbol{g}) - \widehat{\mathcal{R}}_{\mathrm{PLL}}(\boldsymbol{g}) \right| \leq 2\mathfrak{R}_n(\ell_{\mathrm{PLL}} \circ \mathcal{G}) + M\sqrt{\frac{\log(2/\delta)}{2n}}$$

Proof. Consider the one-side uniform deviation $\sup_{\boldsymbol{g}\in\mathcal{G}} \mathcal{R}_{\mathrm{PLL}}(\boldsymbol{g}) - \widehat{\mathcal{R}}_{\mathrm{PLL}}(\boldsymbol{g})$. Since the loss function ℓ is upper-bounded by M, the change of it will be no more than M/n after replacing some x. Then, by *McDiarmid's inequality* (McDiarmid, 1989), for any $\delta > 0$, with probability at least $1 - \delta/2$, the following holds:

$$\sup_{\boldsymbol{g}\in\mathcal{G}} \mathcal{R}_{\mathrm{PLL}}(\boldsymbol{g}) - \widehat{\mathcal{R}}_{\mathrm{PLL}}(\boldsymbol{g}) \leq \mathbb{E}\Big[\sup_{\boldsymbol{g}\in\mathcal{G}} \mathcal{R}_{\mathrm{PLL}}(\boldsymbol{g}) - \widehat{\mathcal{R}}_{\mathrm{PLL}}(\boldsymbol{g}) \Big] + M\sqrt{\frac{\log(2/\delta)}{2n}}.$$

By *symmetrization* (Vapnik, 1998), it is a routine work to show that

$$\mathbb{E}\Big[\sup_{\boldsymbol{g}\in\mathcal{G}} \mathcal{R}_{\mathrm{PLL}}(\boldsymbol{g}) - \widehat{\mathcal{R}}_{\mathrm{PLL}}(\boldsymbol{g}) \Big] \leq 2\mathfrak{R}_n(\ell_{\mathrm{PLL}} \circ \mathcal{G}).$$

The one-side uniform deviation $\sup_{\boldsymbol{g}\in\mathcal{G}} \widehat{\mathcal{R}}_{\mathrm{PLL}}(\boldsymbol{g}) - \mathcal{R}_{\mathrm{PLL}}(\boldsymbol{g})$ can be bounded similarly. □

Then we upper bound $\mathfrak{R}_n(\ell_{\mathrm{PLL}} \circ \mathcal{G})$.

Lemma 4. *Suppose ℓ_{PLL} is defined as Eq. (4), it holds that*

$$\mathfrak{R}_n(\ell_{\mathrm{PLL}} \circ \mathcal{G}) \leq c\mathfrak{R}_n(\ell \circ \mathcal{G}) \leq \sqrt{2}cL_\ell \sum_{y=1}^{c} \mathfrak{R}_n(\mathcal{G}_y).$$

Proof. By definition of ℓ_{PLL}, $\ell_{\mathrm{PLL}} \circ \mathcal{G}(x_i, S_i) = \min_{y \in S} \ell \circ \mathcal{G}(x_i, y) = \min_{y \in [c]} \ell \circ \mathcal{G}(x_i, y)$. Given sample sized n, we first prove the result in the case $c = 2$. The min operator can be written as

$$\min\{z_1, z_2\} = \frac{1}{2}\big[z_1 + z_2 - |z_1 - z_2|\big].$$

In this way, we can write

$$\begin{aligned}
\mathfrak{R}_n(\ell_{\mathrm{PLL}} \circ \mathcal{G}) &= \mathbb{E}_{\boldsymbol{\sigma}}\left[\sup_{\boldsymbol{g}\in\mathcal{G}} \frac{1}{n}\sum_{i=1}^{n} \sigma_i \ell(\boldsymbol{g}(x_i), s_i))\right] \\
&= \mathbb{E}_{\boldsymbol{\sigma}}\left[\sup_{\boldsymbol{g}\in\mathcal{G}} \frac{1}{n}\sum_{i=1}^{n} \sigma_i \min\{\ell(\boldsymbol{g}(x_i), y_1), \ell(\boldsymbol{g}(x_i), y_2)\}\right] \\
&= \mathbb{E}_{\boldsymbol{\sigma}}\left[\sup_{\boldsymbol{g}\in\mathcal{G}} \frac{1}{2n}\sum_{i=1}^{n} \sigma_i \Big[\ell(\boldsymbol{g}(x_i), y_1) + \ell(\boldsymbol{g}(x_i), y_2) - |\ell(\boldsymbol{g}(x_i), y_1) - \ell(\boldsymbol{g}(x_i), y_2)|\Big]\right] \\
&\leq \mathbb{E}_{\boldsymbol{\sigma}}\left[\sup_{\boldsymbol{g}\in\mathcal{G}} \frac{1}{2n}\sum_{i=1}^{n} \sigma_i \ell(\boldsymbol{g}(x_i), y_1)\right] + \mathbb{E}_{\boldsymbol{\sigma}}\left[\sup_{\boldsymbol{g}\in\mathcal{G}} \frac{1}{2n}\sum_{i=1}^{n} \sigma_i \ell(\boldsymbol{g}(x_i), y_2)\right] \\
&+ \mathbb{E}_{\boldsymbol{\sigma}}\left[\sup_{\boldsymbol{g}\in\mathcal{G}} \frac{1}{2n}\sum_{i=1}^{n} \sigma_i \Big|\ell(\boldsymbol{g}(x_i), y_1) - \ell(\boldsymbol{g}(x_i), y_2)\Big|\right] \\
&= \frac{1}{2}\Big(\mathfrak{R}_n(\ell \circ \mathcal{G}) + \mathfrak{R}_n(\ell \circ \mathcal{G})\Big) + \mathbb{E}_{\boldsymbol{\sigma}}\left[\sup_{\boldsymbol{g}\in\mathcal{G}} \frac{1}{2n}\sum_{i=1}^{n} \sigma_i \Big|\ell(\boldsymbol{g}(x_i), y_1) - \ell(\boldsymbol{g}(x_i), y_2))\Big|\right].
\end{aligned} \tag{11}$$

Since $x \mapsto |x|$ is a 1-Lipschitz function, by *Talagrand's contraction lemma* (Ledoux & Talagrand, 2013), the last term can be bounded:

$$\begin{aligned}
&\mathbb{E}_{\boldsymbol{\sigma}}\left[\sup_{\boldsymbol{g}\in\mathcal{G}} \frac{1}{2n}\sum_{i=1}^{n} \sigma_i \Big|\ell(\boldsymbol{g}(x_i), y_1) - \ell(\boldsymbol{g}(x_i), y_2))\Big|\right] \\
\leq &\mathbb{E}_{\boldsymbol{\sigma}}\left[\sup_{\boldsymbol{g}\in\mathcal{G}} \frac{1}{2n}\sum_{i=1}^{n} \sigma_i \Big(\ell(\boldsymbol{g}(x_i), y_1) - \ell(\boldsymbol{g}(x_i), y_2))\Big)\right] \leq \frac{1}{2}\Big(\mathfrak{R}_n(\ell \circ \mathcal{G}) + \mathfrak{R}_n(\ell \circ \mathcal{G})\Big).
\end{aligned} \tag{12}$$

Combining Eq. (11) and Eq. (12) yields $\mathfrak{R}_n(\ell_{\mathrm{PLL}} \circ \mathcal{G}) \leq \mathfrak{R}_n(\ell \circ \mathcal{G}) + \mathfrak{R}_n(\ell \circ \mathcal{G})$. The general case can be derived from the case $c = 2$ using $\min\{z_1, \ldots, z_c\} = \min\{z_1, \min\{z_2, \ldots, z_c\}\}$ and an immediate recurrence.

Then we apply the Rademacher vector contraction inequality (Maurer, 2016),

$$\mathfrak{R}_n(\ell \circ \mathcal{G}) \leq \sqrt{2}L_\ell \sum_{y=1}^{c} \mathfrak{R}_n(\mathcal{G}_y).$$

The proof is completed. □

Table 3. Summary of benchmark datasets and models.

Dataset	# Train	# Test	# Feature	# Class	Model $\boldsymbol{g}(x;\Theta)$
MNIST	60,000	10,000	784	10	Linear model, MLP (depth 5)
Fashion-MNIST	60,000	10,000	784	10	Linear model, MLP (depth 5)
Kuzushiji-MNIST	60,000	10,000	784	10	Linear model, MLP (depth 5)
CIFAR-10	50,000	10,000	3,072	10	ConvNet (Laine & Aila, 2017), ResNet (He et al., 2016)

Based on Lemma 3 and 4, the estimation error bound Eq. (7) is proven through

$$\begin{aligned}
\mathcal{R}_{\mathrm{PLL}}(\widehat{\boldsymbol{g}}_{\mathrm{PLL}}) - \mathcal{R}_{\mathrm{PLL}}(\boldsymbol{g}^*_{\mathrm{PLL}}) &= \Big(\mathcal{R}_{\mathrm{PLL}}(\widehat{\boldsymbol{g}}_{\mathrm{PLL}}) - \widehat{\mathcal{R}}_{\mathrm{PLL}}(\widehat{\boldsymbol{g}}_{\mathrm{PLL}})\Big) + \Big(\widehat{\mathcal{R}}_{\mathrm{PLL}}(\widehat{\boldsymbol{g}}_{\mathrm{PLL}}) - \widehat{\mathcal{R}}_{\mathrm{PLL}}(\boldsymbol{g}^*_{\mathrm{PLL}})\Big) \\
&\quad + \Big(\widehat{\mathcal{R}}_{\mathrm{PLL}}(\boldsymbol{g}^*_{\mathrm{PLL}}) - \mathcal{R}_{\mathrm{PLL}}(\boldsymbol{g}^*)\Big) \\
&\leq \Big(\mathcal{R}_{\mathrm{PLL}}(\widehat{\boldsymbol{g}}_{\mathrm{PLL}}) - \widehat{\mathcal{R}}_{\mathrm{PLL}}(\widehat{\boldsymbol{g}}_{\mathrm{PLL}})\Big) + \Big(\widehat{\mathcal{R}}_{\mathrm{PLL}}(\boldsymbol{g}^*_{\mathrm{PLL}}) - \mathcal{R}_{\mathrm{PLL}}(\boldsymbol{g}^*_{\mathrm{PLL}})\Big) \\
&\leq 2 \sup_{\boldsymbol{g}\in\mathcal{G}} \Big|\mathcal{R}_{\mathrm{PLL}}(\boldsymbol{g}) - \widehat{\mathcal{R}}_{\mathrm{PLL}}(\boldsymbol{g})\Big| \\
&\leq 4\sqrt{2}cL_\ell \sum_{y=1}^{c} \mathfrak{R}_n(\mathcal{G}_y) + 2M\sqrt{\frac{\log(2/\delta)}{2n}}.
\end{aligned}$$

□

D. Supplementary Theorem on Section 4

Theorem 3. *The learning objective in Jin & Ghahramani (2003) is a special case of Eq. (8).*

Proof. Recall the learning objective in Jin & Ghahramani (2003) is formulated as:

$$\widehat{\mathcal{R}}_{\mathrm{PLL}} = \frac{1}{n}\sum_{i=1}^{n} \mathrm{KL}\big[\boldsymbol{z}_i || \boldsymbol{g}(x_i)\big] = \frac{1}{n}\sum_{i=1}^{n} \boldsymbol{z}_i \log \frac{\boldsymbol{z}_i}{\boldsymbol{g}(x_i)}, \tag{13}$$

where KL divergence is used and $\boldsymbol{z}_i$ represents the prior probability of x_i.

Then in Eq. (8), the loss function can be specified as the cross-entropy loss: $\ell_{\mathrm{CE}}(g_j(x_i), e_j^{s_i}) = -e_j^{s_i}\log(g_j(x_i))$, which is linear in the second term, i.e.,

$$\frac{1}{n}\sum_{i=1}^{n}\sum_{j=1}^{c} \mathrm{w}_{ij}\ell_{\mathrm{CE}}(g_j(x_i), e_j^{s_i}) = \frac{1}{n}\sum_{i=1}^{n}\sum_{j=1}^{c} \ell_{\mathrm{CE}}(g_j(x_i), \mathrm{w}_{ij}e_j^{s_i}).$$

Thus, the weights $\mathbf{w}$ can be moved into the loss function and yields:

$$\widehat{\mathcal{R}}_{\mathrm{PLL}} = \frac{1}{n}\sum_{i=1}^{n}\sum_{j=1}^{c} \ell_{\mathrm{CE}}(g_j(x_i), z_{ij}) = -\frac{1}{n}\sum_{i=1}^{n} \boldsymbol{z}_i \log \boldsymbol{g}(x_i), \tag{14}$$

where $z_{ij} = \mathrm{w}_{ij}\mathbb{I}(j \in s_i)$. The optimal $\boldsymbol{g}^*$ of Eq. (14) is essentially equivalent to $\boldsymbol{g}^*$ learned from Eq. (13). Therefore, our method is a strict extension of (Jin & Ghahramani, 2003). □

E. Benchmark Datasets

E.1. Setup

Tabel 3 describes the benchmark datasets and the corresponding models of them.

MNIST This is a grayscale image dataset of handwritten digits from 0 to 9 where the size of the images is 28×28.

The linear model is a linear-in-input model: d-10, and MLP refers to a 5-layer FC with ReLU as the activation function: d-300-300-300-300-10. Batch normalization (Ioffe & Szegedy, 2015) was applied before hidden layers. For both models, the softmax function was applied to the output layer, and ℓ_2-regularization was added. The two models were trained by SGD with the default momentum parameter ($\beta = 0.9$), and the batch size was set to 256.

Fashion-MNIST This is a grayscale image dataset similarly to MNIST. In Fashion-MNIST, each instance is a 28×28 grayscale image and associated with a label from 10 fashion item classes. The models and optimizer were the same as MNIST.

Kuzushiji-MNIST This is another grayscale image dataset similarly to MNIST. In Kuzushiji-MNIST, each instance is a 28×28 grayscale image and associated with a label from 10 cursive Japanese (Kuzushiji) characters. The models and optimizer were the same as MNIST.

CIFAR-10 This dataset consists of 60,000 $32 \times 32 \times 3$ colored image in RGB format in 10 classes.

The detailed architecture of ConvNet (Laine & Aila, 2017) is as follows.

0th (input) layer:	(32*32*3)-
1st to 4th layers:	[C(3*3, 128)]*3-Max Pooling-
5th to 8th layers:	[C(3*3, 256)]*3-Max Pooling-
9th to 11th layers:	C(3*3, 512)-C(3*3, 256)-C(3*3, 128)-
12th layers:	Average Pooling-10

where C(3*3, 128) means 128 channels of 3*3 convolutions followed by Leaky-ReLU (LReLU) active function (Maas et al., 2013), [·]*3 means 3 such layers, etc.

The detailed architecture of ResNet (He et al., 2016) was as follows.

0th (input) layer:	(32*32*3)-
1st to 11th layers:	C(3*3, 16)-[C(3*3, 16), C(3*3, 16)]*5-
12th to 21st layers:	[C(3*3, 32), C(3*3, 32)]*5-
22nd to 31st layers:	[C(3*3, 64), C(3*3, 64)]*5-
32nd layer:	Average Pooling-10

where [·, ·] means a building block (He et al., 2016). These two models were trained by SGD with the default momentum parameter and the batch size was 256.

An example of a binomial flipping with $q = 0.1$ and of a pair flipping with $q = 0.5$ used on MNIST are below, respectively:

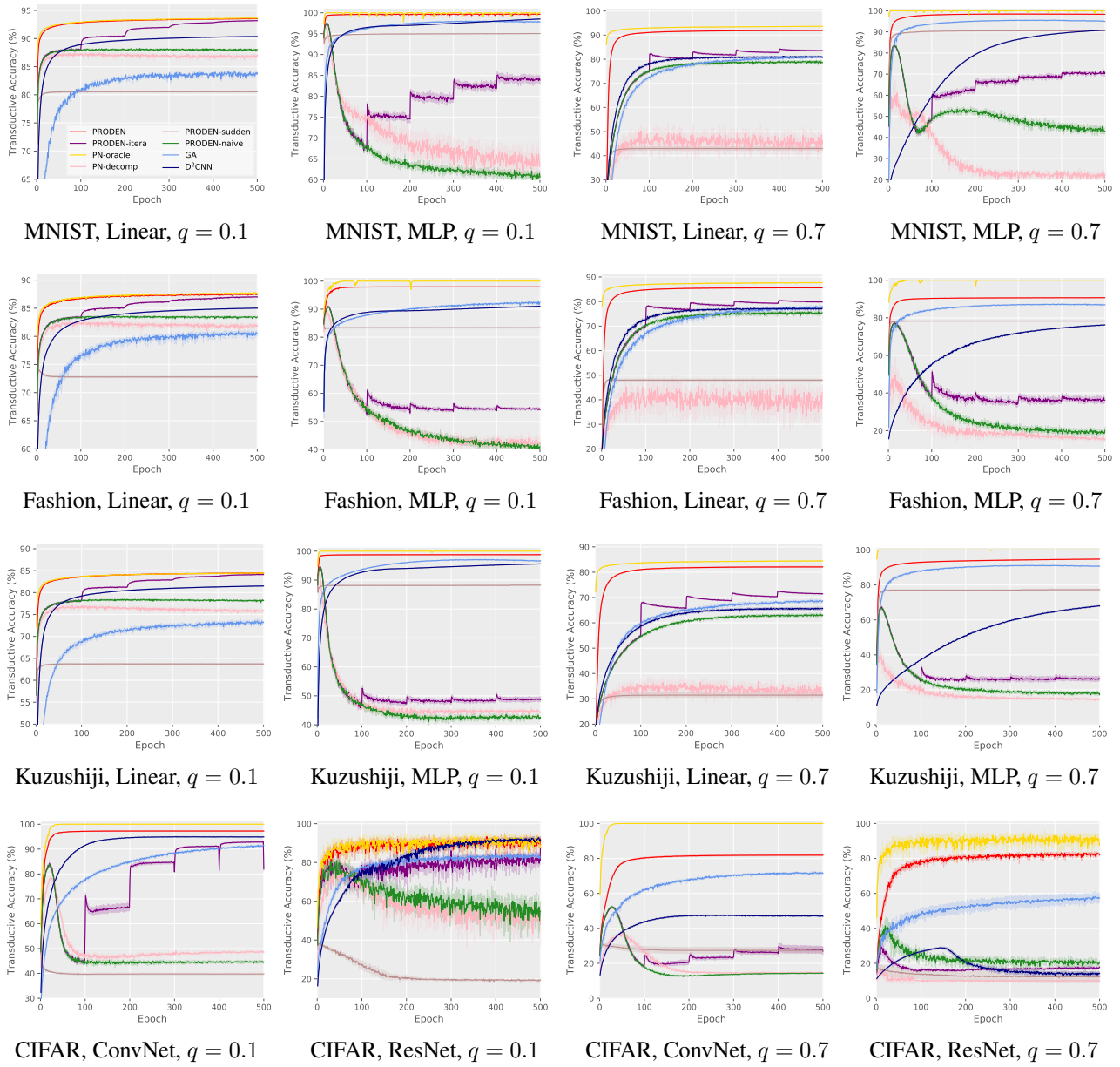
$$\begin{bmatrix} 1 & 0.1 & 0.1 & 0.1 & 0.1 & 0.1 & 0.1 & 0.1 & 0.1 & 0.1 \\ 0.1 & 1 & 0.1 & 0.1 & 0.1 & 0.1 & 0.1 & 0.1 & 0.1 & 0.1 \\ 0.1 & 0.1 & 1 & 0.1 & 0.1 & 0.1 & 0.1 & 0.1 & 0.1 & 0.1 \\ 0.1 & 0.1 & 0.1 & 1 & 0.1 & 0.1 & 0.1 & 0.1 & 0.1 & 0.1 \\ 0.1 & 0.1 & 0.1 & 0.1 & 1 & 0.1 & 0.1 & 0.1 & 0.1 & 0.1 \\ 0.1 & 0.1 & 0.1 & 0.1 & 0.1 & 1 & 0.1 & 0.1 & 0.1 & 0.1 \\ 0.1 & 0.1 & 0.1 & 0.1 & 0.1 & 0.1 & 1 & 0.1 & 0.1 & 0.1 \\ 0.1 & 0.1 & 0.1 & 0.1 & 0.1 & 0.1 & 0.1 & 1 & 0.1 & 0.1 \\ 0.1 & 0.1 & 0.1 & 0.1 & 0.1 & 0.1 & 0.1 & 0.1 & 1 & 0.1 \\ 0.1 & 0.1 & 0.1 & 0.1 & 0.1 & 0.1 & 0.1 & 0.1 & 0.1 & 1 \end{bmatrix} \quad \begin{bmatrix} 1 & 0.5 & 0 & 0 & 0 & 0 & 0 & 0 & 0 & 0 \\ 0 & 1 & 0.5 & 0 & 0 & 0 & 0 & 0 & 0 & 0 \\ 0 & 0 & 1 & 0.5 & 0 & 0 & 0 & 0 & 0 & 0 \\ 0 & 0 & 0 & 1 & 0.5 & 0 & 0 & 0 & 0 & 0 \\ 0 & 0 & 0 & 0 & 1 & 0.5 & 0 & 0 & 0 & 0 \\ 0 & 0 & 0 & 0 & 0 & 1 & 0.5 & 0 & 0 & 0 \\ 0 & 0 & 0 & 0 & 0 & 0 & 1 & 0.5 & 0 & 0 \\ 0 & 0 & 0 & 0 & 0 & 0 & 0 & 1 & 0.5 & 0 \\ 0 & 0 & 0 & 0 & 0 & 0 & 0 & 0 & 1 & 0.5 \\ 0.5 & 0 & 0 & 0 & 0 & 0 & 0 & 0 & 0 & 1 \end{bmatrix}$$

E.2. Transductive Results

Figure 3 illustrates the transductive results on the benchmark datasets, i.e., the ability in identifying the true labels in the training set. We can see that PRODEN has a strong ability to find the true labels.

E.3. Test Results in the Pair Case

Figure 4 illustrates the test results on the benchmark datasets in the pair case. They show a similar phenomenon to Figure 2 that PRODEN is affected slightly and CCN is affected severely when the ambiguity degree goes large.



MNIST, Linear, $q = 0.1$ | MNIST, MLP, $q = 0.1$ | MNIST, Linear, $q = 0.7$ | MNIST, MLP, $q = 0.7$

Fashion, Linear, $q = 0.1$ | Fashion, MLP, $q = 0.1$ | Fashion, Linear, $q = 0.7$ | Fashion, MLP, $q = 0.7$

Kuzushiji, Linear, $q = 0.1$ | Kuzushiji, MLP, $q = 0.1$ | Kuzushiji, Linear, $q = 0.7$ | Kuzushiji, MLP, $q = 0.7$

CIFAR, ConvNet, $q = 0.1$ | CIFAR, ResNet, $q = 0.1$ | CIFAR, ConvNet, $q = 0.7$ | CIFAR, ResNet, $q = 0.7$

Figure 3. Transductive accuracy for various models and datasets. Dark colors show the mean accuracy of 5 trials and light colors show standard deviation. Fashion is short for Fashion-MNIST, Kuzushiji is short of Kuzushiji-MNIST, CIFAR is short of CIFAR-10.

F. UCI datasets

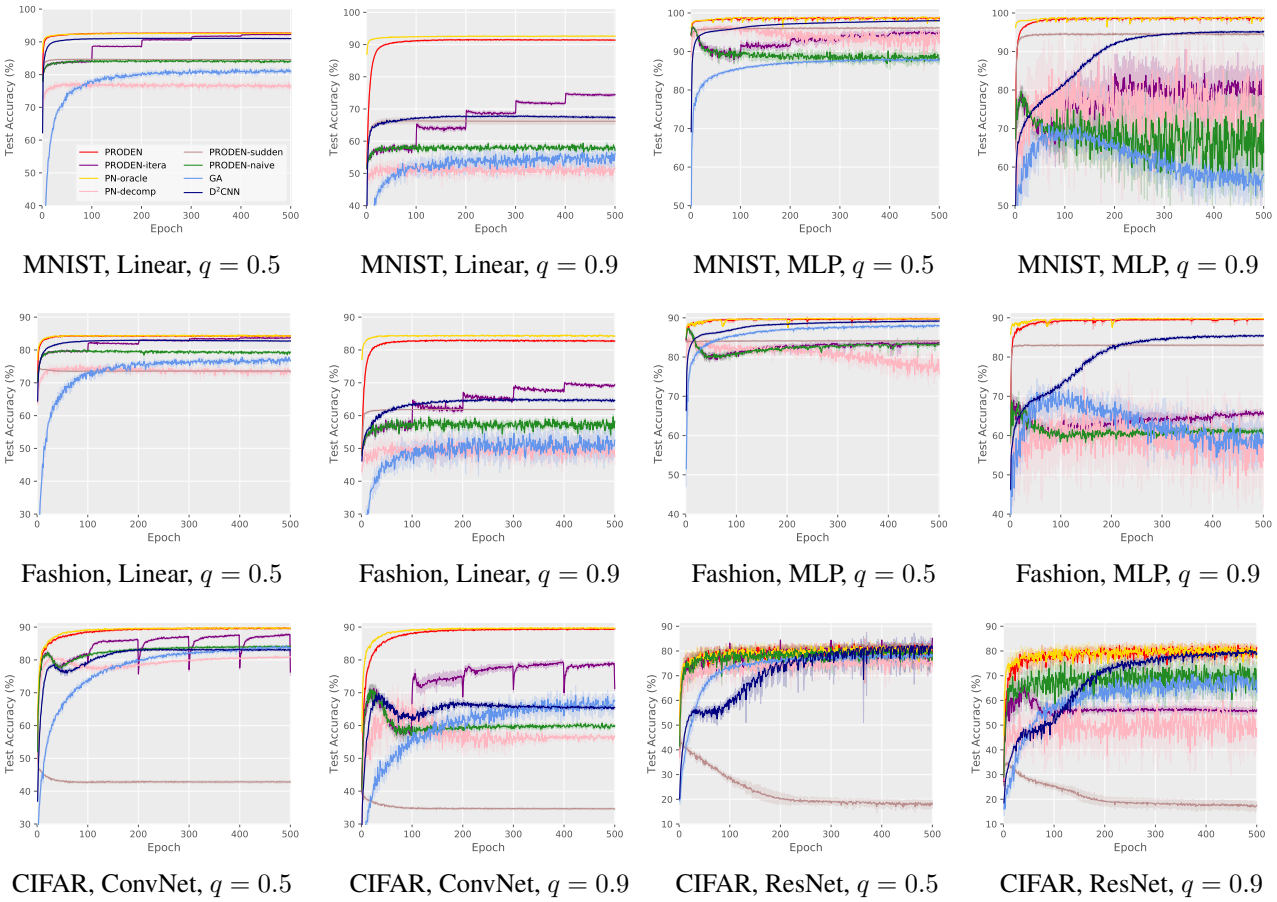
F.1. Characteristic of the UCI Datasets and Setup

Table 4 summaries the characteristic of the UCI datasets. We normalized these dataset by the Z-scores by convention and use the linear model trained by SGD with momentum 0.9.

F.2. Comparing Methods

The comparing PLL methods are listed as follows.

- *SURE* (Feng & An, 2019a): an iterative EM-based method [suggested configuration: $\lambda, \beta \in$



MNIST, Linear, $q = 0.5$ | MNIST, Linear, $q = 0.9$ | MNIST, MLP, $q = 0.5$ | MNIST, MLP, $q = 0.9$

Fashion, Linear, $q = 0.5$ | Fashion, Linear, $q = 0.9$ | Fashion, MLP, $q = 0.5$ | Fashion, MLP, $q = 0.9$

CIFAR, ConvNet, $q = 0.5$ | CIFAR, ConvNet, $q = 0.9$ | CIFAR, ResNet, $q = 0.5$ | CIFAR, ResNet, $q = 0.9$

Figure 4. Test accuracy on MNIST, Fashion-MNIST, and CIFAR-10 in the pair case.

$\{0.001, 0.01, 0.05, 0.1, 0.3, 0.5, 1\}$].

- *CLPL* (Cour et al., 2011): a parametric method that transforms the PLL problem to the binary learning problem [suggested configuration: SVM with squared hinge loss].
- *ECOC* (Zhang et al., 2017): a disambiguation-free method that adapts the binary decomposition strategy to PLL [suggested configuration: $L = log_2(l)$].
- *PLSVM* (Nguyen & Caruana, 2008): a SVM-based method that differentiates candidate labels from non-candidate labels by maximizing the margin between them [suggested configuration: $\lambda \in \{10^{-3}, \ldots, 10^{3}\}$].
- *PLkNN* (Hullermeier & Beringer, 2006): a non-parametric approach that adapts k-nearest neighbors method to handle partially labeled data [suggested configuration: $k \in \{5, 6, \ldots, 10\}$].
- *IPAL* (Zhang & Yu, 2015): a non-parametric method that applies the label propagation strategy to iteratively update the weight of each candidate label [suggested configuration: $\alpha = 0.95, k = 10, T = 100$].

F.3. Results

Tabel 5 provides additional experiments to investigate the performances of each comparing methods on the UCI datasets with the pair flipping strategy. It shows that PRODEN generally achieves superior performance against other parametric comparing methods. Our advantage is a less obvious compared with the non-parametric method IPAL, whereas the performance of PRODEN could be easily increased by employing a deeper network.

Table 4. Summary of UCI datasets and models.

Dataset	# Train	# Test	# Feature	# Class	Model $\boldsymbol{g}(x;\Theta)$
Yeast	1,335	149	8	10	Linear model
Texture	4,950	550	40	11	Linear model
Dermatology	329	37	34	6	Linear model
Synthetic-Control	540	60	60	6	Linear model
20Newsgroups	16,961	1,885	300	20	Linear model

Table 5. Test accuracy (mean±std) on the UCI datasets in the pair case.

	q	Yeast	Texture	Dermatology	Synthetic Control	20Newsgroups
PRODEN	0.5	**56.38±4.71%**	**99.71±0.12%**	**96.16±3.27%**	98.05±1.58%	78.05±0.97%
	0.9	**44.03±4.12%**	**99.35±0.31%**	93.68±6.80%	96.33±1.12%	**70.71±0.72%**
PRODEN-itera	0.5	56.26±4.74%	99.13±0.40%•	93.15±2.56%	87.40±7.25%•	76.90±0.92%
	0.9	42.62±5.52%	78.74±4.09%•	68.14±6.89%•	57.90±5.08%•	57.15±0.71%•
GA	0.5	24.39±4.40%•	94.25±0.48%•	73.81±6.18%•	64.68±3.08%•	63.68±0.67%•
	0.9	16.50±3.43%•	61.85±2.29%•	48.03±11.42%•	37.15±6.91%•	45.86±0.95%•
D^2CNN	0.5	56.38±4.71%	98.71±0.28%•	95.89±3.75%	78.87±11.94%•	74.38±0.90%•
	0.9	41.52±7.03%	86.45±4.87%•	87.84±6.58%	62.92±12.36%•	64.16±0.36%•
SURE	0.5	51.69±3.81%	98.18±0.17%•	95.71±2.49%	78.67±5.26%•	70.21±0.88%•
	0.9	37.61±3.40%•	98.00±0.42%•	93.42±6.23%	52.33±6.49%•	61.01±0.93%•
CLPL	0.5	55.06±4.74%	98.80±0.22%•	94.52±3.36%	75.83±4.29%•	77.92±0.76%
	0.9	40.66±4.69%	90.21±4.77%•	87.67±3.06%	52.33±4.65%•	65.03±0.32%•
ECOC	0.5	54.55±3.92%	99.47±0.17%•	94.71±2.29%	96.67±2.08%	**78.67±1.11%**
	0.9	42.51±5.19%	69.69±4.82%•	92.97±6.61%	94.50±1.32%	70.11±1.63%
PLSVM	0.5	52.59±2.04%	93.38±2.22%•	93.97±4.50%	91.83±3.08%•	76.21±2.30%
	0.9	41.89±3.90%	82.24±6.58%•	93.15±4.22%	80.67±9.42%•	70.76±2.16%
PLkNN	0.5	53.60±2.81%	97.11±0.28%•	94.52±3.06%	94.83±2.60%•	43.77±0.72%•
	0.9	43.80±4.50%	92.98±0.64%•	92.05±4.38%	89.83±4.54%•	38.77±0.90%•
IPAL	0.5	51.80±5.08%	99.30±0.37%	95.89±2.74%	**98.50±1.37%**	76.83±0.51%
	0.9	36.60±2.58%•	98.95±0.58%•	**95.34±2.29%**○	**98.50±1.09%**○	69.15±0.73%

G. Characteristic of the Real-world Datasets and Setup

Tabel 6 summarizes the characteristic of the real-world datasets and the corresponding models. The preprocessing, model and optimizer were the same as UCI datasets.

Table 6. Summary of real-world partial label datasets.

Dataset	# Examples	# Feature	# Class	# Avg. CLs	Task Domain	Model $\boldsymbol{g}(x;\Theta)$
Lost	1122	108	16	2.23	automatic face naming (Panis & Lanitis, 2014)	Linear model
BirdSong	4998	38	13	2.18	bird song classification (Briggs et al., 2012)	Linear model
MSRCv2	1758	48	23	3.16	object classification (Liu & Dietterich, 2012)	Linear model
Soccer Player	17472	279	171	2.09	automatic face naming (Zeng et al., 2013)	Linear model
Yahoo! News	22991	163	219	1.91	automatic face naming (Guillaumin et al., 2010)	Linear model